

# Investigations on the stability of the low pressure positive column in oxygen

H Testrich<sup>1</sup>, D Pasedag<sup>1</sup>, Z Navrátil<sup>2</sup>, B May<sup>1</sup>, R Reimer<sup>1</sup>, C Wilke<sup>3</sup> and H-E Wagner<sup>1</sup>

<sup>1</sup> Institute of Physics, University of Greifswald, F.-Hausdorff-Str. 6, D-17489 Greifswald, Germany

<sup>2</sup> Department of Physical Electronics, Faculty of Science, Masaryk University, Kotlářská 2, CZ-611 37 Brno, Czech Republic

<sup>3</sup> INP Greifswald (Leibniz-Institute for Plasma Science and Technology), F.-Hausdorff-Str. 2, D-17489 Greifswald, Germany

E-mail: [wagner@physik.uni-greifswald.de](mailto:wagner@physik.uni-greifswald.de)

Received 6 February 2009, in final form 13 May 2009

Published 3 July 2009

Online at [stacks.iop.org/JPhysD/42/145207](http://stacks.iop.org/JPhysD/42/145207)

## Abstract

The stability of the low pressure positive column in oxygen was investigated in a pressure range from 0.5 to 0.9 Torr within a discharge current interval from 0.5 to 90 mA. The transition between the well-known T- and H-modes has been studied. The H- to T-mode transition showed a marked hysteresis in the  $E(I)$  characteristic which is affected by wall processes. For the first time temporally resolved electric field measurements were realized. At small discharge current the electric field showed a significant modulation, characterized by incoherent fluctuations with a broadband Fourier spectrum. With increasing current the discharge operates in the T-mode, where a mode selection with high modulation degree occurred, resulting in a periodic oscillation of the electric field at a discrete frequency spectrum. The dynamic state in the T-mode is expressed by T-waves moving from the cathode to the anode. It seems that they were excited by oscillations in the cathode region. The waves were damped in the direction of the anode and show no dispersion.

The discharge stability was studied using a hydrodynamic model considering electrons, positive and negative ions as well as metastable  $O_2(a^1\Delta_g)$  molecules. Here the negative  $O^-$ -ions play a crucial role. In good agreement with the experiments the transition between the H- and T-modes was explained as a linear unstable equilibrium state where the energy dependence of the corresponding rate coefficients is the driving mechanism (attachment-induced instability).

(Some figures in this article are in colour only in the electronic version)

## 1. Introduction

Molecular plasmas show a large variety of instabilities which lead to the excitation of different nonlinear patterns, as standing and moving striations or the constriction of plasmas [1]. This is especially true in electronegative gases, where negative ions drastically change the local plasma properties. They play a basic role in the excitation of instabilities and structurization which express dynamic operation states of the plasma. The instabilities are correlated with non-uniform electric fields, particle densities and local gas heating. Despite considerable progress, we are far from an adequate understanding of these

complex correlations. This requires investigations which link the observed instabilities to the relevant plasma species and their reactions.

Observations on instabilities in electronegative gases have a long history. For many years they have already been studied in the positive column of low pressure oxygen glow discharges, e.g. [2–5] or, for example, in  $SF_6$  [6]. Recent measurements focused on the quantitative diagnostics of  $O^-$  ions, mainly realized by photo-detachment and probe measurements [7, 8]. Investigations in  $O_2$ -rf-afterglow plasmas have allowed important insights into the processes [8, 9]. Because the application of negative ions under stable

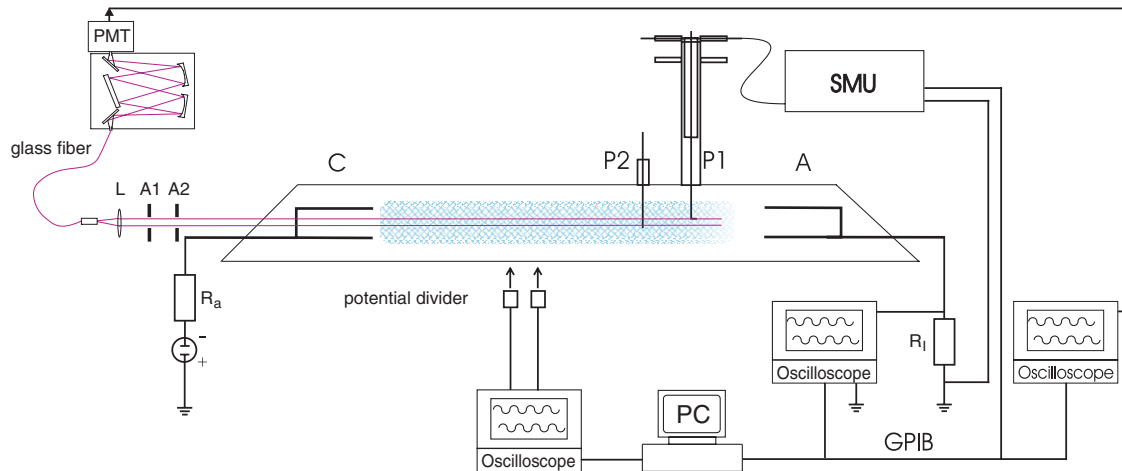


**Figure 1.** Experimental set-up. SMU—source measure unit, PMT—photomultiplier, C—cathode, A—anode, P1/2—probes, L—lens and A1/2—apertures.

plasma conditions is of high interest in plasma technology, such investigations are of practical relevance, too [10, 11].

The illustrated situation motivated the authors to come back to former measurements in the positive column of low pressure oxygen dc glow discharges [5, 12] and to pick up questions which have not been answered up to now. The progress in the technical equipment allows both a sensitive detection of stability/instability as well as the diagnostics of relevant species (negative ions and metastable oxygen molecules). They provide the experimental database for theoretical efforts, to correlate the instabilities with relevant particles on the basis of kinetic models [13].

The positive column in oxygen operates in two modes, the so-called H-mode with a higher average electric field strength and the T-mode with a low average electric field ('T' in German 'Tief') [2, 5], traditionally detected by static voltmeters, only. In contrast, our temporally resolved field measurements will show a complex dynamic behaviour behind this. In particular, the T-mode is characterized by different kinds of dynamic operation states, besides others, the so-called T-waves. These waves have a phase velocity in the cathode to anode direction (forward waves) and show no dispersion [5]. A long-standing problem is the deeper understanding of the transition between these two operation modes, i.e. the transition from the homogeneous plasma to instabilities.

In the paper we discuss the results of our instability investigations. It is organized as follows. In section 2 the experimental set-up is described and details of the applied diagnostic methods are discussed. Next, experimental results on the T- and H-modes of the discharge operation are presented in section 3. In particular, averaged measurements of the electric field strength, the hysteresis in the transition between both modes and the dynamic behaviour of the electric field are presented (section 3.1). The characterization of the wave phenomena, namely, their frequency spectra, phase velocity of T-waves and dispersion, are summarized in section 3.2. The sensitive indication of the operation modes by the gas temperature is discussed in section 3.3. Here selected results on the spectroscopic determination of the rotational temperature from the oxygen molecules and

their comparison with the solution of heat balance equation are given. In section 4 some experimental data for the T- to H-mode transition are compared with the results of theoretical investigations on the stability of the dc oxygen discharge [13].

## 2. Experimental set-up

In figure 1 the experimental set-up is shown. The discharges operated in closed glass tubes with an inner diameter of 50 mm and a distance between the cylindrical electrodes of 600 mm. New tubes have been prepared with the usual heating procedure under high vacuum before the measurements, followed by a longer discharge burn-in in pure oxygen (purity better than 99.995 vol%). The open cylindrical electrodes (made of pure aluminium) allowed radially resolved measurements as well as the detection of the axial discharge radiation.

The dc positive column has been operated in a pressure range from 0.5 to 0.9 Torr within a discharge current interval from 0.5 to 90 mA. For the discharge operation high voltage power supplies from FUG (type HCN 350-3500) have been used.

The dynamical states (standing striations, waves) were recorded in two ways<sup>4</sup>.

- A diode array consisting of 128 diodes with a spatial resolution of 0.5 cm allowed to detect the spatio-temporally resolved light emission of the whole positive column.
- Because the waves produce electric potential alterations, their propagation was recorded with two potential dividers located outside at the tube wall. This second technique is very useful especially at the weak light emission of the oxygen plasma.

Their frequency spectra were visualized by a FFT Spectrum Analyzer (type SR760 from Stanford Research Systems). The axial electric field strength was measured by two Langmuir probes (distance 50 mm, material: platinum or tungsten).

<sup>4</sup> The coincidence of both methods was proved by the comparative investigation of the column plasma in Ne which has a high radiation intensity.

Under stable discharge conditions, the probes allowed the estimation of density and energy of the plasma electrons. One of the probes (P1) could be shifted across the tube diameter and enabled radially resolved measurements. From the molecular oxygen emission it was possible to determine its rotational temperature which is in good approximation equal to the gas temperature. The radiation was recorded with an ARC Spectra Pro 750 monochromator. It was taken from a cylindrical region along the whole discharge tube by means of two iris diaphragms, mounted at the discharge axis between the hollow anode and optical fibre (cf figure 1). Since no molecular radiation was registered in the cathode glow, only radiation coming from the positive column was studied in this configuration.

Additionally, the set-up was configured to detect negative ions by laser detachment of their electrons. For this a pulsed solid state laser with a wavelength of 532 nm (detachment of  $O^-$  ions) is directed on the Langmuir probe P1. The changes in the probe current by the detached electrons are correlated quantitatively with the negative ion density. That is why plane entrance windows of the discharge tube were used. They were fixed with an angle of around  $40^\circ$  to avoid reflections of the radiation back to the laser resonator.

To avoid any misunderstanding, it is noted that the probe measurements of electrons and negative ions as well as their radial profiles are still in progress. The results will be published later.

### 3. Experimental results and discussion

#### 3.1. The H- and T-mode of the positive column in oxygen

As a first step, the existence ranges of the discharge operation modes were detected in the traditional manner: the temporal averaged axial potential gradients were measured across the two probes by static voltmeters. The H- and T-modes appear at constant filling pressures  $p_0$  with variation of the discharge current  $I$ . They are characterized by significantly different average electric fields  $E$  and have been classified by Sabadil [5]. The transition between the different modes is associated with the external electrical circuit (namely the series resistor) as well as the properties of the column itself (cf section 4). Considering former results, high enough resistor values had to be used to prevent the influence of the external circuit on the transition ranges [12]. Under our conditions this was the case for resistors of 50–70 k $\Omega$ . In figure 2 a typical  $E(I)$  characteristic is shown. At small discharge currents high averaged  $E$  fields are detected. Therefore, this operation mode was named in the older literature as the H-mode, too [5]. Because of its marked modulation (see below) we will rename this range as the  $H^*$ -mode. With increasing current, the well known falling  $E(I)$  characteristics of the positive column are observed. Then the T-mode appears, connected with a pronounced dynamic behaviour and an extreme modulation degree. With rising current the column jumps into the H-mode, characterized by small plasma modulations or homogeneous discharge conditions. In qualitative agreement with former results, this second transition shows a considerable hysteresis

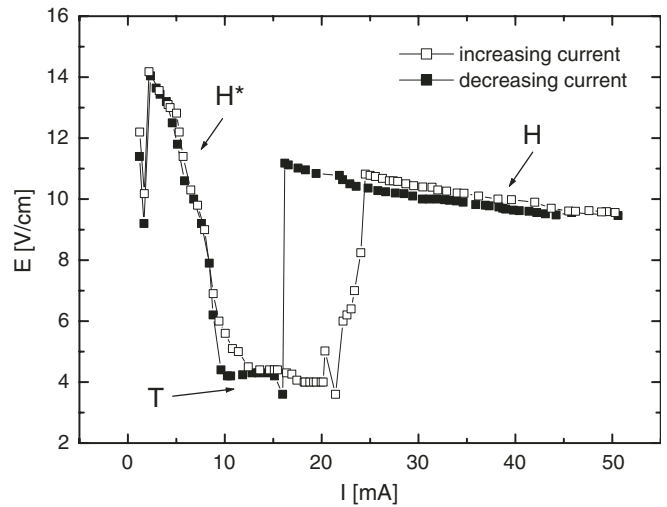


**Figure 2.** Axial electric field strength  $E$  in dependence on the discharge current  $I$  and the hysteresis at static measurements for increasing and decreasing current. Conditions:  $p_0 = 0.5$  Torr oxygen.

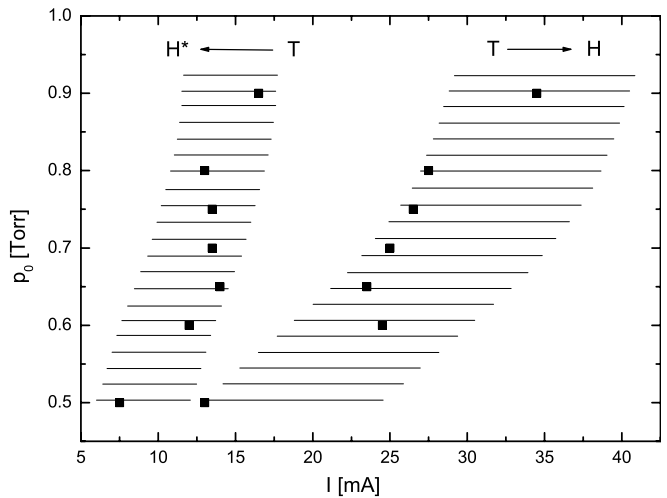


**Figure 3.** Pressure dependence of the H-mode and T-mode. Filled squares: measurements within some days in a new tube; the hachures summarize all measurements in different discharge tubes over a long period.

for increasing and decreasing discharge current which is typical for strong nonlinear systems (figure 2). The higher the filling pressure the more the jumps  $T \rightarrow H$  are shifted to higher discharge currents, and the windows of the T-mode are wider. These measurements are summarized in figure 3. The jumps from the T-mode to the H-mode (detected with increasing current) as well as the transition back  $T \rightarrow H^*$  (measured for decreasing current) are shown here. In a newly prepared discharge tube and within a small time interval, the measurements have a good reproducibility (cf figure 3, filled squares). But, summarizing all measurements in different discharge tubes over a longer period, there is a variation/shift of the ranges (figure 3, hachures). Of course, the qualitative behaviour remains the same! These results underline the importance of wall processes, significantly affecting the discharge operation modes and, therefore, the

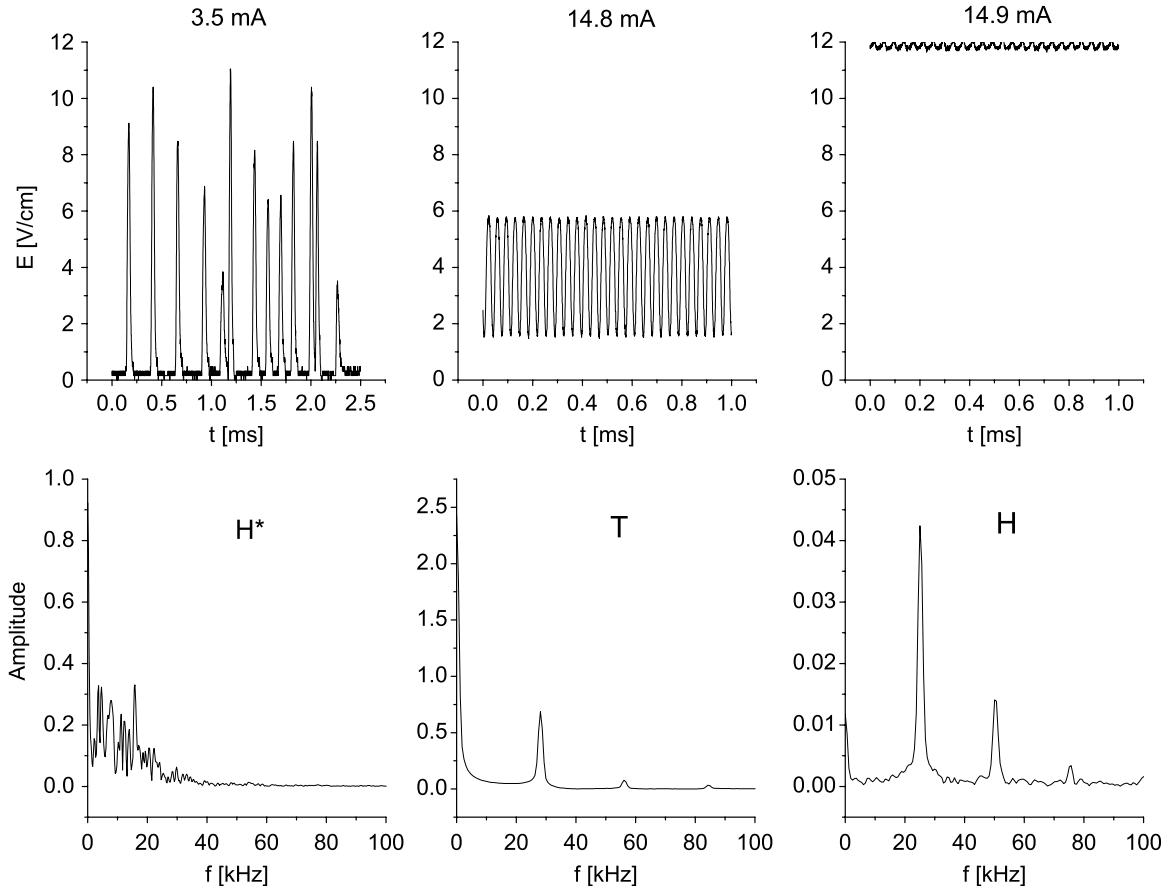
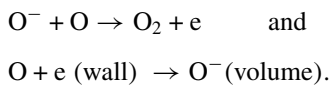


**Figure 4.** Temporally resolved measurement of the axial electric field  $E$  for the  $H^*$ -, T- and H-modes with increasing current as well as the corresponding frequency spectra (experimental conditions:  $p_0 = 0.7$  Torr oxygen,  $r_0 = 25$  mm; the probes are placed about 10 cm from the anode).

ranges of instabilities. Such investigations have already been reported many years ago [3]. Taking into account the crucial role of negative ions in the formation of instabilities, we have to find out reactions having an effect on their density by wall processes. Possible channels are, e.g.,



It is known that the recombination coefficient of O-atoms and the efficiency of negative ion formation at the wall depend sensitively on the glass type and/or deposited layers (e.g. by electrode sputtering).

In particular, in the T-mode we observed a high modulation of the discharge current which is caused by different discharge instabilities. Therefore, temporally resolved measurements of the electric field in the oxygen column are required. For the first time, they were realized by two frequency compensated potential dividers which allowed the detection of frequencies up to 30 kHz. They were connected to two probes (distance 50 mm), placed 100 mm away from the anode. It should be noted that in the studied (new) discharge tube of identical geometry the T-mode covered only a very narrow current window—somewhat different from the results shown in figure 3. But, this fact does not influence the general insights on the discharge dynamics. In figure 4 typical results

for the pressure  $p_0 = 0.7$  Torr are shown. Surprisingly, the discharge operation at small discharge current ( $H^*$ -mode, too) is characterized by incoherent fluctuations of the field with a broadband Fourier spectrum (noise or chaotic state). Only because of the high time constant of static voltmeters, a voltage close to the maxima is recorded. By increasing the current, a mode selection (with a high modulation degree) occurs resulting in a periodic oscillation of the electric field and a discrete frequency spectrum. As discussed above, this is the T-mode with low averaged electric fields (here about  $3.7 \text{ V cm}^{-1}$ )<sup>5</sup>. At higher discharge currents the discharge jumps into the H-mode, characterized by higher values of the electric field (here about  $12 \text{ V cm}^{-1}$ ), and a discrete frequency spectrum with small modulation degree which is comparable to the modulation degree of moving striations in noble gases [14, 15]. In the H-mode there is a transition to the homogeneous column for higher discharge currents. If only maximum values of the electric field in the  $H^*$ - and T-modes are considered, the  $E(I)$  dependence corresponds to the static measurements.

<sup>5</sup> The observed dynamical behaviour in the positive column of an oxygen glow discharge is similar to the formation of striations in the positive column of a neon glow discharge: via Hopf bifurcation a wave mode develops from a noise spectrum by changing the current [16].

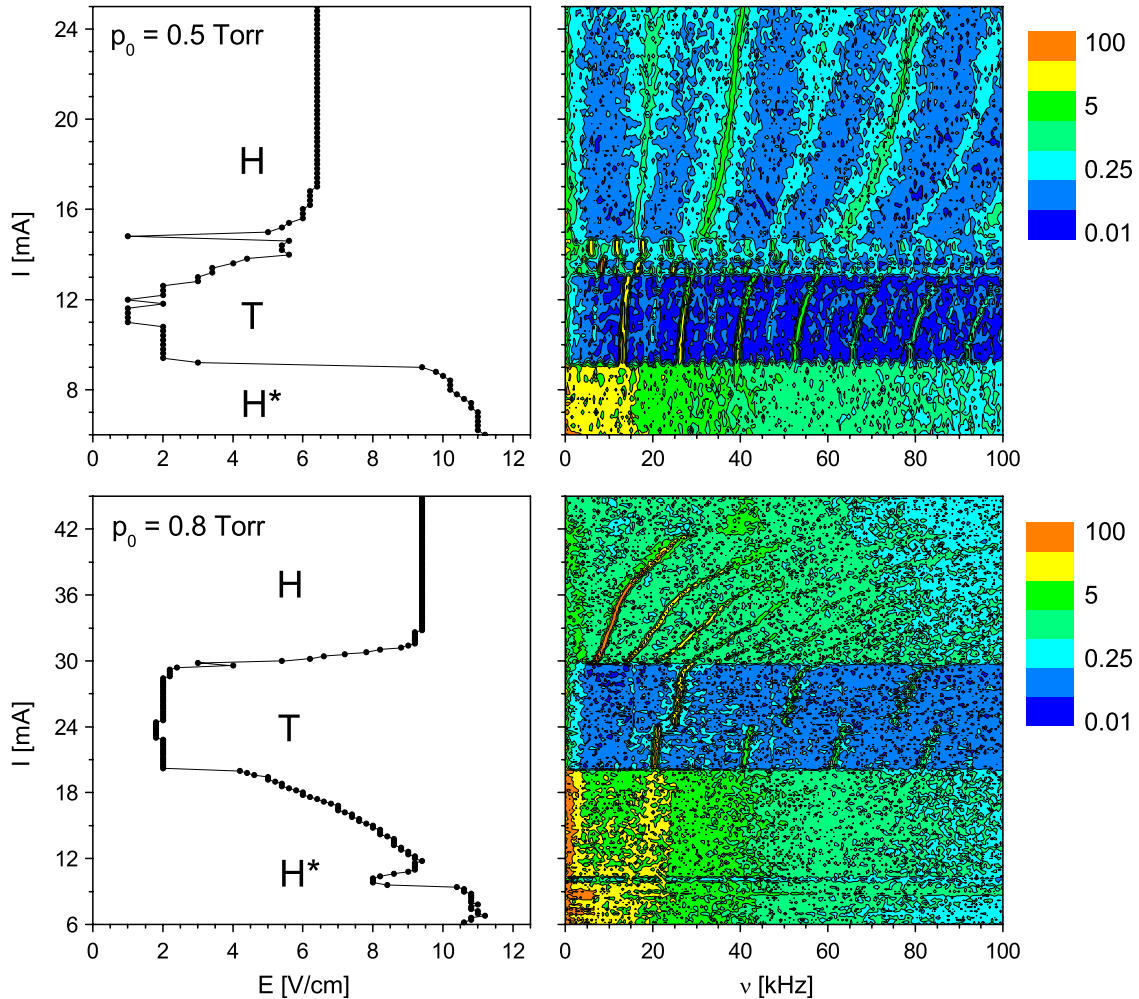


**Figure 5.** Averaged electric field (static voltmeter) depending on the discharge current for two oxygen filling pressures and detected frequency spectra. Scale of relative intensity.

### 3.2. The wave phenomena

In contrast to former measurements [5], in this investigation the waves were recorded without any external synchronization/excitation. In most cases potential dividers, placed near the tube wall, were applied for the sensitive spatio-temporally detection of wave phenomena in dependence on the discharge current as control parameter. We focused on T-waves (forward waves, moving from the cathode to the anode) in the T-mode of discharge operation and the detection of instabilities in the transition range to the H-mode. Typical results are summarized in figure 5 for the filling pressures  $p_0 = 0.5$  and 0.8 Torr. The detected frequency spectra (fundamental frequencies, higher harmonics) are shown together with the averaged electric fields in the different discharge modes.

Starting at small discharge currents (H\*-mode) one observes for both pressures noise spectra (yellow band) (cf section 3.1). With increasing current a mode selection occurs before the transition to the H-mode. This can be clearly seen in figure 5 for 0.8 Torr. Next, there is a transition to the T-mode, characterized by T-waves with discrete frequency spectra (fundamentals, higher harmonics). The fundamental frequencies start at about 13 kHz (0.5 Torr)

and 20 kHz (0.8 Torr) and increase slightly with the discharge current (yellow traces/lines). Within the T-mode sometimes a mode change in the frequency spectra can be detected (figure 5, 0.8 Torr, 24 mA) which is not understood up to now. The transition from the T- to the H-mode is triggered by small disturbances/instabilities of the column. As a reason for the transition here a secondary bifurcation can be assumed: in the first step a period-doubling is induced. This state is unstable and via a period-3-bifurcation (second step) the final transition from the T- to the H-mode takes place. This scenario can be seen very clearly at 0.5 Torr in the current interval 13–15 mA. This small range is shown magnified in figure 6. But it has been observed in the whole studied pressure range<sup>6</sup>. Within the H-mode moving striations of small modulation can be investigated. For higher discharge currents the column operates under homogeneous conditions. Surprisingly, the averaged electric field reflects sensitively all the discussed transitions.

An example for the spatio-temporal propagation of the T-waves is given in figure 7. As already described in section 2, these measurements were realized with two potential dividers,

<sup>6</sup> Similar scenarios were studied in Ne columns, too [17].

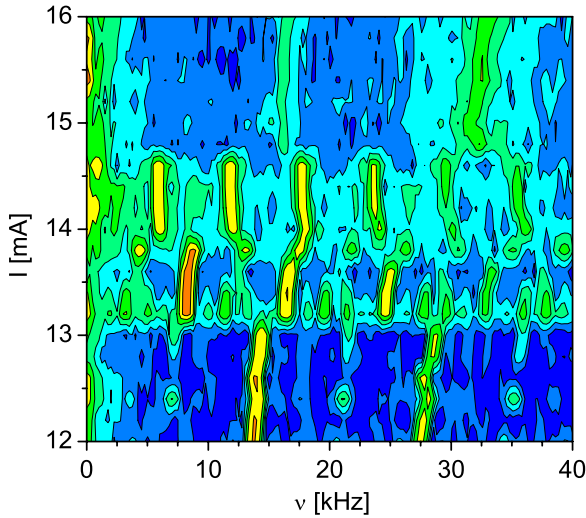


**Figure 6.** Magnified current range of the T- to H-mode transition at 0.5 Torr from figure 5. Identical scale of relative intensity.

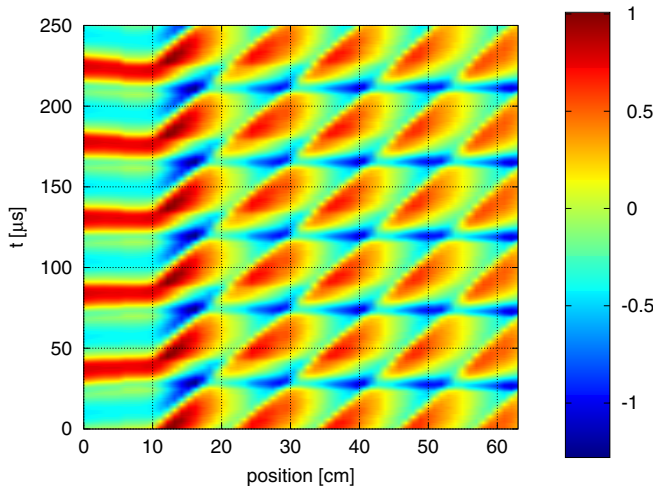


**Figure 7.** Spatio-temporally propagation of T-waves, moving from the cathode to the anode. Scale of relative intensity. Conditions:  $p_0 = 0.7$  Torr  $O_2$ ,  $I = 11.6$  mA,  $v = 2.5 \times 10^5$  cm s<sup>-1</sup>,  $f = 21.4$  kHz,  $\lambda = 12.0$  cm.

too. One of the dividers was located at a fixed position of the positive column producing a stable trigger signal for the oscilloscope. The second one was moved stepwise along the tube wall between the cathode and the anode in this way recording the wave propagation. In the cathode region (distance  $\leq 10$  cm) oscillations of high amplitude are observed. These oscillations seem to excite the waves in the positive column which move from the cathode to the anode. Under the experimental conditions of figure 7, the waves have a phase velocity of  $2.5 \times 10^5$  cm s<sup>-1</sup>. Their wavelength is 12 cm. Generally, it slightly depends on the discharge current and pressure, respectively. The space–time diagram shows ‘bubbles’ (intensity variation) which propagate from the cathode to the anode. The formation of this space–time diagram can be interpreted as a superposition of an amplitude modulated wave with an oscillation of the same frequency. Therefore, these wave phenomena seem to be not self-excited. It is remarkable that they are damped in the direction of the

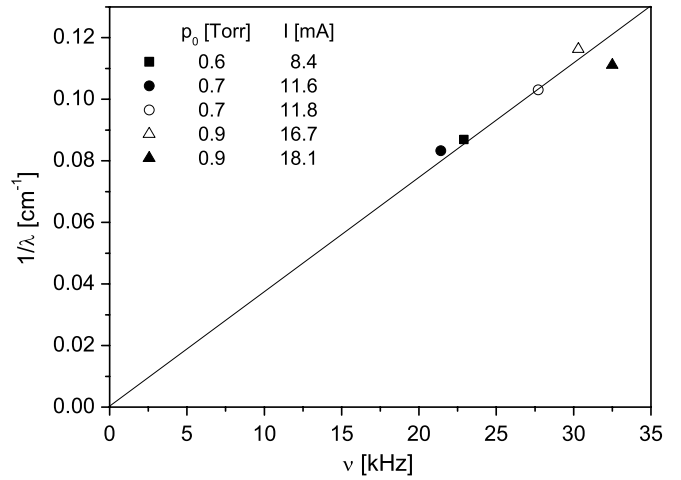


**Figure 8.** Reciprocal T-wavelengths in dependence on the fundamental frequencies for different operation conditions.

anode. In agreement with former measurements, the T-waves show no dispersion. This is illustrated in figure 8 for different discharge conditions. The reciprocal wavelengths are linearly dependent on the fundamental frequencies. A common phase velocity of  $2.5 \times 10^5 \pm 1.4 \times 10^4$  cm s<sup>-1</sup> was determined, which is in good agreement with former results [5]. Up to now it is not obvious what kind of mechanism is responsible for the formation and propagation of the waves with high degree of modulation. It needs further verification. GUNN instabilities, striations and ion-acoustic waves were discussed [18]. In several theoretical investigations the T-mode is linked to attachment-induced instabilities, e.g. [13, 19, 20]. Already in [20] the importance of the radial profiles of the electron density is discussed. It is expected that our current radially resolved measurements of the relevant species of the positive column will contribute to a deeper understanding. Temporally resolved measurements of the relevant species under non-stationary conditions would be necessary, too. This is a hard challenge for future investigations.

### 3.3. The gas temperature in H- and T-modes

It was found that the neutral gas temperature is evidently a sensitive indicator of the discharge operation modes as well as the T–H hysteresis. In this section selected investigations are summarized. Its direct determination is usually complicated. Therefore, a spectroscopic measurement of the rotational temperature of  $O_2$  molecules was carried out. It can be simply determined from the rotational structure of molecular emission, in this work from the rotational distribution of  $O_2$  molecules in the  $b^1\Sigma_g^+$  excited state. The rotational temperature of this state is generally considered as a good approximation of the kinetic temperature of  $O_2$  molecules in the ground state [21]. Because of the low radiation intensity of the oxygen column, we adopted a powerful method which enables the determination of rotational temperature from the band profile with unresolved rotational structure [22].

The radial resolution of the temperature profiles was about 5 mm. In the measurements of the current dependences of the rotational temperature, a wider discharge region ( $\approx 1$  cm)

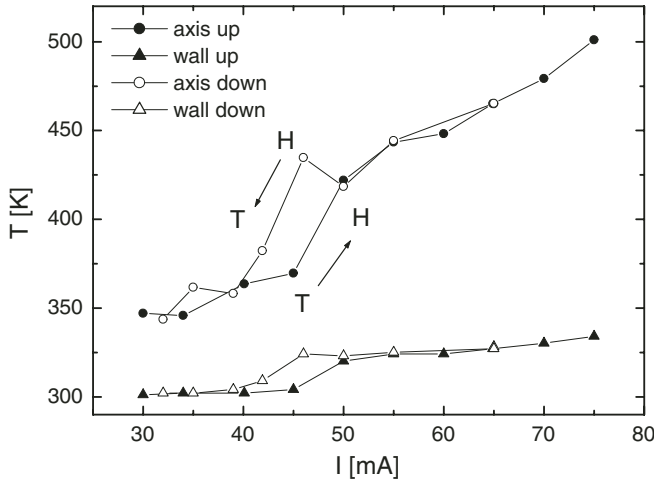


**Figure 9.** Rotational (gas) temperature (on top) and wall temperature (down) in dependence on the discharge current. Measurement ‘up’: increasing current, ‘down’: decreasing current. Condition:  $p_0 = 0.7$  Torr oxygen.

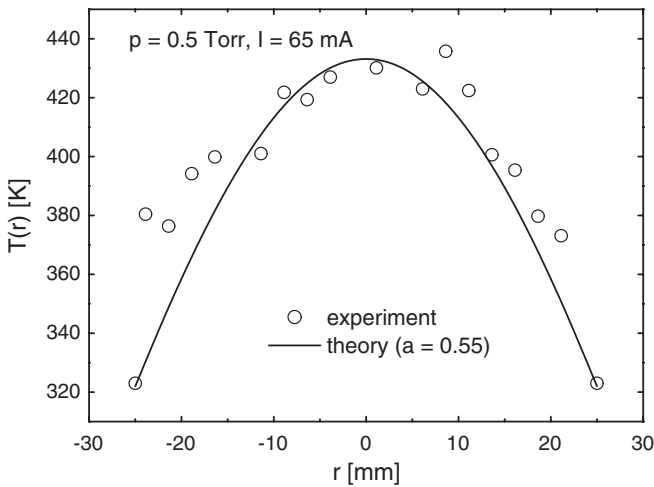


**Figure 10.** Radial profile of neutral gas temperature for 0.5 Torr oxygen, 65 mA,  $r_0 = 25$  mm. The fraction  $a = 0.55$  of invested power is converted into heat.

around the axis was analysed. The establishment of radial heat transfer after individual current change was monitored by the registration of wall temperature with thermocouples. Usually, the temperature became stable within several minutes of operation after the current change.

In figure 9 the gas temperature in the discharge axis and the wall temperature in dependence on the discharge current are shown. The measurements were performed for increasing and decreasing current. Remarkable differences for both operation modes have been recorded. The T–H hysteresis can be observed both in rotational (gas) temperature and in wall temperature. The differences correspond to the different power dissipation in H- and T-modes in the positive column. An example of the radial temperature profiles is shown in figure 10. The measurements are in quite good agreement with the calculated values, solving the heat transfer equation. Under the assumptions of axial homogeneity and radial symmetry of

the column it is given by

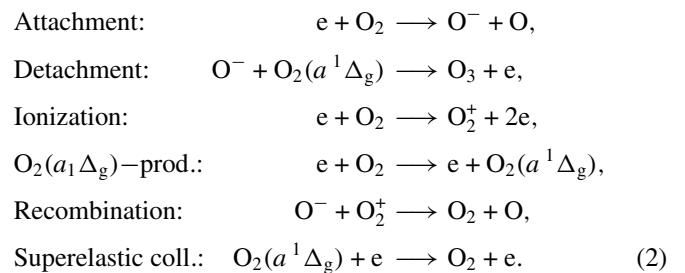
$$aEj(r) = \frac{1}{r} \partial_r [r\lambda \partial_r T(r)], \quad (1)$$

where  $a$  is the fraction of electric power converted to heat (adaptation to experimental temperature profile),  $E$  is the axial electric field (taken from the experiment),  $j(r)$  is the axial current density with radial profile, mainly transported by electrons of the density  $n_e$  (adapted by experiment),  $\lambda = \lambda(300 \text{ K}) = 0.024 \text{ W m}^{-1} \text{ K}^{-1}$ : heat conductivity of oxygen,  $T(r)$  is the temperature profile, with  $T(r_0) = T_{\text{wall}}$  and  $I = 2\pi \int_0^{r_0} rj(r) dr$  is the discharge current. The radial  $n_e(r)$  distribution was approximated by a Gaussian profile  $n_e \sim \exp(-\eta r^2)$  with  $\eta = 0.1 \text{ cm}^{-2}$  (adapted by the experiment). Of course, other profiles could be used, too, leading to the same final results. Under the conditions of figure 9 about 55% of the invested electric power ( $a = 0.55$ ) is converted into heat!

#### 4. Comparison with theoretical results

In this section we compare some of our experimental results with theoretical investigations on the stability of the dc oxygen discharge. The detailed theoretical investigations are published in [13]. Therefore, we do not repeat the complete theoretical description and stability analysis. For clarity, here only a brief survey of the underlying physical model of the positive column is given.

As a first step, the theoretical description tries to investigate the existence of self-excited waves and their properties in the positive column. According to the plasma parameter region a hydrodynamical model was used with a reduction to a minimal set of plasma species. The used components are electrons (e), negative ions ( $\text{O}^-$ ), positive ions ( $\text{O}_2^+$ ) and metastable oxygen molecules ( $\text{O}_2(a^1\Delta_g)$ ). Other species such as  $\text{O}^+$  or  $\text{O}_2^-$  or other excited oxygen states have comparatively lower concentrations (see, e.g. [23]) and are therefore neglected. The following reaction channels were included in the model:



Since the mean electron energy controls many plasma processes, the energy balance is included in the fluid model. As the experimental analysis delivers axial time depending effects, radial perturbations are neglected and a cross-section averaging for the particle densities without any angular dependences is performed. For the radial profiles BESSEL functions (see [24] or [25] for motivation) with free parameters  $\lambda_e$  for the electrons,  $\lambda_n$  for the negative ions and  $s$  as a sticking probability for the metastable oxygen molecules (see [13] for details) are used. A radial energy loss at the wall is modelled effectively with the help of another free model parameter  $\Lambda_U$ .

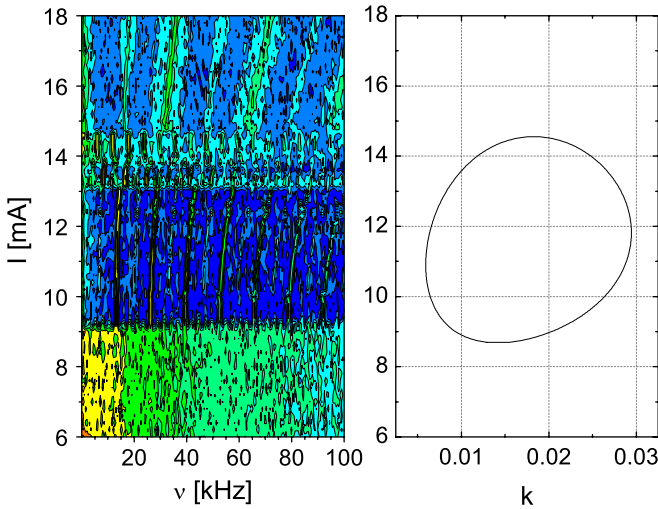


**Figure 11.** Detected frequency spectra depending on the discharge current in the different operation modes (conditions:  $p_0 = 0.5$  Torr oxygen,  $r_0 = 25$  mm) (left) and calculated stability boundaries for the discharge current  $I$  and the dimensionless wave number  $k$  for  $\lambda_e = 1.22$ – $1.61$ ,  $\lambda_n = 0.01$ ,  $\Lambda_u = 2.8$  (right).

For a quantification of the equilibrium state experimental input is necessary. Those are on the one hand the macroscopic model parameters current  $I$ , pressure  $p$ , temperature  $T$  and the wall temperature  $T_w$ , and on the other hand mainly the electric field measurements so that the intrinsic model parameters from the radial ansatz can be set. The temperature values are taken from measurements of the rotational temperature (see section 3.3) and the electric field from the  $E(I)$  characteristic measurements (see figure 2).

For the system of balance equations linear stability analysis can be done (technical details can be seen in [13]). In the theoretical model a linear stable equilibrium state corresponds to the H-mode of the discharge. In figure 11 a theoretical stability calculation was made for 0.5 Torr. Here the loop defines a stable and an unstable discharge regime. All waves with a corresponding wave number  $k$  within the loop are linear unstable and will grow up in time. The maximum and minimum of the loop define a characteristic wave for one certain wave number  $k$  where the discharge changes into a linear unstable regime. These are the so-called critical points. The occurring bifurcation here is a so-called HOPF bifurcation. The calculated linear wavelength and frequencies deviate from the experimental results. This could be caused by a nonlinear shift of the wave phenomena after a subcritical HOPF bifurcation [13]. Interestingly, a homogeneous discharge regime can be found for low currents. This is in contrast to the experimental results which are presented here, where a dynamical state for low currents can be observed (H\*-mode (see section 3.2)). The position of the instability window with respect to the current depends on the sticking probability of the metastable molecules and the width of the window can be varied by means of the energy wall loss (described by model parameter  $\Lambda_U$ ) [13]. The dependence on the energy is very sensitive and it is possible that the experimentally observed variations of the windows (cf figure 3) are a consequence of small electron energy variations.

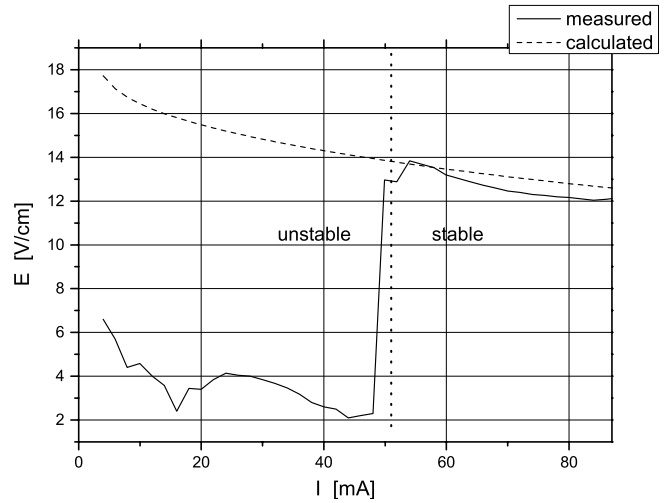


**Figure 12.** Measured and calculated electric field  $E$  as a function of discharge current  $I$  at 0.85 Torr. Vertical broken line: calculated instability boundary. The used radial parameters are  $\lambda_e = 0.65$ – $0.8$ ,  $\lambda_n = 0.01$ ,  $s = 5.4 \times 10^{-4}$  and  $\Lambda_U = 4.5$ . The temperature  $T$  was varied from 300 to 550 K.

Figure 12 shows a similar calculation for a higher pressure. The homogeneous discharge equilibrium is linearly unstable, i.e. there is no stable region at small currents. This result is in better agreement with our experimentally observed H\*-mode as a dynamical state. Therefore, the result of  $p = 0.85$  Torr seems to support the fact that the hydrodynamical models work better in higher than in lower pressure regions.

The hysteresis shown in figure 2 cannot be discussed in the context of linear stability analysis because it is a nonlinear effect. However, the theoretically found HOPF bifurcation (see [13]) provides an indication because it arises in two different cases. In the so-called subcritical case one observes a hard onset of the wave dynamics and the system jumps into a highly nonlinear state. As a rule, this type of transition is connected with hysteresis. Indeed, current research activities could prove that at the higher current boundary a subcritical HOPF bifurcation takes place [26].

A similar situation arises for our experimentally observed transition from the T- to the H\*-mode or for the period-3-bifurcation discussed in section 3.2, which are secondary bifurcations within a strong nonlinear region where linear analysis is not a proper description. These nonlinear phenomena must be studied numerically with a fully nonlinear hydrodynamical model where especially the role of negative ions will be in focus. The influence of the external circuit including current feedback and oscillations at the cathode is also a further step. Up to now it is not fully understood which role the cathode region plays for the development of the instabilities in the positive column.

Although, there are many open questions connected with the strong nonlinear character of the oxygen discharge, the presented model shows good agreement in the qualitative behaviour of the plasma. A quantitative agreement is a challenging task for further investigations. Up to now a complete theoretical picture of axial and radial phenomena is not available. But it was also possible to get a first idea

of the crucial role of negative ions for the development of the instability. The basic mechanism in this model is the attachment-induced instability, where the energy dependence of attachment and ionization rate coefficient play the dominant role [13, 19, 20].

## 5. Conclusions

- The low pressure positive column in oxygen operates in the long time known H- and T-modes which are characterized by quite different (averaged) electric field strengths. In contrast to former static investigations, a significant modulation of the axial electric field in the different operation modes was recorded for the first time. The discharge operation at small discharge current (traditionally named H-mode, too!) is characterized by incoherent fluctuations of the field with a broadband Fourier spectrum. Therefore, it was renamed H\*-mode. With increasing current, a mode selection (with high modulation degree) occurs resulting in a periodic oscillation of the electric field and a discrete frequency spectrum. This is the T-mode with low averaged electric field. At higher discharge currents the discharge jumps into the H-mode with higher values of the electric field and a discrete frequency spectrum with small modulation degree.
- The H- to T-mode transition shows a marked hysteresis in the  $E(I)$  characteristic. The existence range is significantly affected by wall processes.
- Up to now it is not obvious what kind of mechanism is responsible for the formation and propagation of the T-waves with a high degree of modulation. Under the experimental conditions studied, they seem to be excited by oscillations in the cathode region, and they are damped in the direction of the anode. In good agreement with former results, these waves show no dispersion and propagate with a phase velocity of  $2.5 \times 10^5 \text{ cm s}^{-1}$  from the cathode to the anode. Their wavelength is about 12 cm, slightly depending on the discharge current and pressure.
- For the transition from the T- to the H-mode a secondary bifurcation can be assumed: in the first step a frequency jumping is induced by a side band instability. This state is unstable and (in a second step) via a period-3-bifurcation the final transition from the T- to the H-mode takes place.
- A deeper understanding of the formation of T-waves requires temporally resolved measurements of the relevant species (electrons,  $\text{O}^-$ -atoms and metastable molecules) under non-stationary conditions. This will be a hard challenge for the future.
- The gas temperature is evidently a sensitive indicator of the discharge operation modes as well as of the T–H hysteresis.
- The discharge stability has been studied using a hydrodynamic model considering the relevant particles and reaction channels. Here the negative  $\text{O}^-$ -ions play a crucial role. In good agreement with the experiments the transition between the H- and T-modes was explained as a linear unstable equilibrium state where the energy

dependence of the corresponding rate coefficients is the driving mechanism (attachment-induced instability).

- Further theoretical investigations will try to analyse the dynamical behaviour of the full nonlinear model. With the help of numerical investigations it might be possible to calculate the spectra and investigate the striations. So the effective plasma processes can be extracted for a full understanding of the development of the plasma instability and especially the role of the negative ions. Future analytical observations can validate the occurrence of the subcritical HOPF bifurcation so that a theoretical explanation for the hysteresis can be found.

## Acknowledgments

The authors express their gratitude to R Zweier for her excellent technical support and systematic measurements on the discharge instabilities. They thank M Bogaczyk very much for programming LabVIEW and the visualization of the data by MATLAB. Furthermore, the authors express their deep gratitude to B Bruhn and A Richter for their helpful support and the excellent cooperation within the common project. This work was supported by the ‘Deutsche Forschungsgemeinschaft’ in the frame of the Sonderforschungsbereich TRR-24 ‘Fundamentals of complex plasmas’, project B1 and supported by research project MSM0021622411 of the Ministry of Education of the Czech Republic.

## References

- [1] Garscadden A 1978 Ionization waves in glow discharges *Gaseous Electronics* vol 1 ed M N Hirsch and H J Oscam (New York: Academic)
- [2] Seeliger R and Wichmann A 1953 *Z. Naturf.* **8a** 74
- [3] Seeliger R 1953 *Z. Naturf.* a **8** 74
- [4] Rutscher A and Wojacek K 1964 *Beitr. Plasmaphys.* **1–2** 41
- [5] Sabadil H 1966 *Beitr. Plasmaphys.* **6** 305
- [6] Ishikawa I, Matsumoto M and Suganomata S 1984 *J. Phys. D: Appl. Phys.* **17** 85
- [7] Amemiya H 1985 *Vacuum* **58** 100
- [8] Katsch H M, Manthey C and Döbele H F 2003 *Plasma Sources Sci. Technol.* **12** 475
- [9] Katsch H M, Sturm T and Döbele H F 2000 *Plasma Sources Sci. Technol.* **9** 323
- [10] Stoffels E 2004 *10th Int. Symp. on Gaseous Dielectrics (Athens, Greece)* (invited lecture)
- [11] Liebermann M A and Lichtenberg A J 1994 *Principles of Plasma Discharges and Materials Processing* (New York: Wiley-Interscience)
- [12] Sabadil H 1968 *Beitr. Plasmaphys.* **8** 299
- [13] Bruhn B, Richter A and May B 2008 *Phys. Plasmas* **15** 053505
- [14] Rademacher K and Wojacek K 1958 *Ann. Phys., Lpz.* **415** 57
- [15] Wojacek K and Novak M 1962 *Beitr. Plasmaphys.* **3** 1–11
- [16] Dinklage A, Wilke C and Klinger T 1999 *Phys. Plasmas* **6** 2968
- [17] Golubowski Yu, Skoblo A Yu, Wilke C, Kozakov R V, Behnke J and Nekuchaev V O 2005 *Phys. Rev. E* **72** 026414
- [18] Sabadil H 1971 *Beitr. Plasmaphys.* **11** 327
- [19] Nighan W L and Wiegand W J 1974 *Phys. Rev. A* **10** 922
- [20] Vikharev A L, Ivanov O A, Yu Kuznetsov O and Stepanov A N 1989 *Sov. J. Plasma Phys.* **15** 485

- [21] Touzeau M, Vialle M, Zellagui A, Gousset G and Lefevre M 1991 *J. Phys. D: Appl. Phys.* **24** 41
- [22] Macko P and Veis P 1999 *J. Phys. D: Appl. Phys.* **32** 246
- [23] Richter A, Testrich H, Wagner H-E, Loffhagen D and Wilke C 2009 *J. Plasma Phys.* **75** 71–84
- [24] Arutunyan G G, Galechyan G A and Tavakalyan L B 1983 *Beitr. Plasmaphys.* **23** 271
- [25] Franklin R N 2001 *J. Phys. D: Appl. Phys.* **34** 1834  
Franklin R N and Snell J 1999 *J. Phys. D: Appl. Phys.* **32** 2190
- [26] Bruhn B 2009 private communication